THEORY OF FLUORESCENCE POLARIZATION IN MAGNETICALLY ORIENTED PHOTOSYNTHETIC SYSTEMS

ROBERT S. KNOX AND MARIA A. DAVIDOVICH, *Department of Physics and Astronomy, and Institute for Fundamental Studies, University of Rochester, Rochester, New York 14627 U. S. A.*

ABSTRACT Many cells and cell fragments are known to assume specific alignments with respect to an applied magnetic field. One indicator of this alignment is a difference between the intensities of fluorescence observed in polarizations parallel and perpendicular to the magnetic field. We calculate these two intensities using a model that assumes axially symmetric membranes and that covers a wide variety of shapes from flat disk to right cylinder. The fluorescence is assumed to originate at chromophores randomly excited but nonrandomly oriented in the membranes. The membrane alignment is assumed to be due to the net torque on a nonrandom distribution of diamagnetically anisotropic molecules. The predicted results are consistent with most magnetoorientation data from green cells, but we are able to show that *Chlorella* data are not consistent with the hypothesis that the membranes have, and maintain, a cup-like configuration.

INTRODUCTION

A. Overview

Optical properties of materials have long provided valuable insights into structures and mechanisms. Using them as a tool on biological cells has generally meant a compromise between, on the one hand, maintaining physiological conditions in which the optical effects are made isotropic by randomness and motion, and, on the other hand, establishing some orientation by artificial means, even to the extent of freezing and sectioning. Recently, it has been found that magnetic fields of moderate intensity can be used to orient single cells in a natural physiological environment with no apparent destructive effect. Optical properties of magnetically oriented samples are anisotropic, and thus the usefulness of optical measurements for structure analysis in vivo has been regained to a certain extent.

In this article we present an analysis the primary purpose of which is the correlation of the observed fluorescence anisotropy with a model involving assumed local orientations of the relevant molecules within membranes having a variety of possible shapes. The fluorescence is taken to originate in chromophores with nondegenerate states

Dr. Davidovich's present address is: Departmento de Fisica, Pontifica Universidade Católica, Rio de Janeiro, Brazil.

radiating in dipole-allowed transitions, as is appropriate for chlorophyll. The chromophores are assumed randomly excited, as they would be after absorption and fairly extensive energy transfer; i.e., in this paper we do not carry out a theory of the intrinsic polarization anisotropy.

In the remainder of this introduction we discuss the history of the magnetic orientation of cells (part B), the currently accepted biophysical basis of the effect (part C), and a summary of the procedures we will adopt (part D). In section II a general method of characterizing axial membrane distributions is developed and a shape parameter defined. In section III we show how the shape and local diamagnetic anisotropy combine to produce specific orientations in the field. Section IV contains the prediction of the optical anisotropy and a discussion designed especially to elucidate the interesting case of *Chlorella*. After the concluding remarks (section V), three appendices provide some computational details.

B. Background

During a search for magnetic field effects on the delayed fluorescence in *Chlorella* cells, Geacintov and co-workers (1) discovered a surprisingly large field dependence in the normal fluorescence characteristics. The circumstances of this discovery are worth recalling.

Triplet exciton collision probabilities are very sensitive to magnetic fields because the magnetic sublevels are split and shifted by the field, affecting initial sublevel populations and densities of final states. As in the case of simple Zeeman effects, the observed spectral changes therefore originate at the molecular level and may be called "microscopic" effects. Stacy and co-workers (2) had sought to test the idea that triplet exciton collisions were involved in the production of delayed light in photosynthesis, in analogy to the well-known effects in crystals of aromatic molecules (see, e.g., references 3 and 4 for general reviews). They had found no effect for fields up to 18 kG, and Geacintov was attempting the experiment at higher fields. The changes he actually found in the normal fluorescence could be explained in terms of the orientation of entire cells by the field, with no reference to the energy level structure—a "macroscopic" effect. To our knowledge microscopic effects of the type mentioned above have yet to be observed in vivo, although evidence for various exciton collisions under high excitation intensity is accumulating (5), and the effects of magnetic fields on the population of chlorophyll triplet states in preparations from biological systems have been observed at low temperatures (6).

Magnetic orientation of biological systems had already been observed visually by Arnold et al. (7), who oriented muscle fibers, and by Chalazonitis et al. (8), who oriented retinal rod segments and found that osmotic or heat shock would destroy the orientation. In the *Chlorella* work, the primary finding was that the fluorescence yield (1) and polarization (9) depended on the orientation of the field with respect to the direction of propagation and/or polarization of the absorbed and emitted light. Since the original discovery, visual (10), X-ray (11), and neutron scattering (12) observation of the magnetic orientation of photosynthetic particles has been reported, and

extensive refinement of the analysis of the effect for use as a tool in deducing pigment orientations on membranes in various photosynthetic cells has been made (13–17).

C. *Mechanism of Orientation*

To place our present work in context, we give a brief description of the experiments and their general explanation as developed by Geacintov and co-workers. Fluorescence was viewed in a direction perpendicular to the field, the dominant contribution coming from the ~685 nm chlorophyll *a* fluorescence band. The exciting light beam was oriented perpendicular to both the magnetic field and the fluorescence viewing direction but with its polarization parallel to the field. The fluorescence polarized perpendicular to the field, $F_{\perp}(H)$, increased with the field, whereas that parallel to the field, $F_{||}(H)$, decreased (9; Fig. 1). This indicated that, in the magnetic field, the chlorophylls are oriented in such a way that the transition moment of the lowest electronic transition (the "red" chlorophyll band) tends to lie in a plane perpendicular to the field. The fluorescence polarization ratio, $F_{\perp}(H)/F_{||}(H)$, was found to vary with different strains of *Chlorella* as well as with different cultures of the same strain. In the original work (9, 13, 15), one *Chlorella* strain gave values from 1.30 to 1.57, whereas another gave 1.10, at a magnetic field of 10.5 kG, corresponding to saturation. More recently, Becker (16) has found a value of 1.9. The fluorescence polarization suggested that magnetic field-induced dichroism in the main absorption band, at 675–578 nm, should also occur. This was indeed observed.

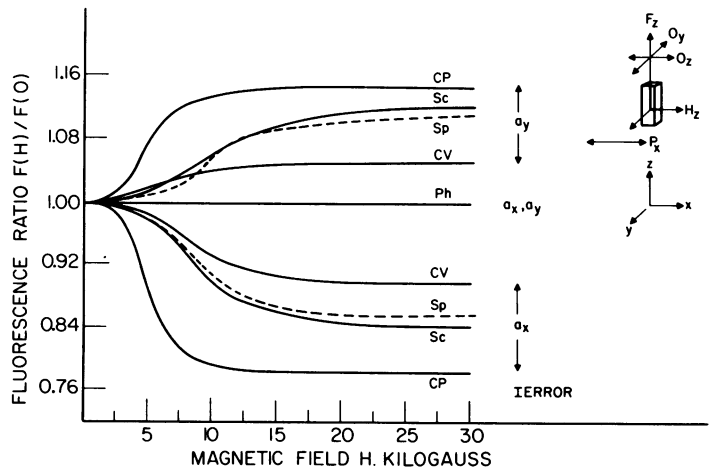

FIGURE 1 Polarized fluorescence of chlorophyll *a* in vivo as a function of magnetic field strength. $F(H)$, fluorescence intensity in the magnetic field H; $F(0)$, zero field fluorescence; F_z, fluorescence viewing direction; a_x, a_y, analyzer orientation either parallel or perpendicular to H; $h\nu$, direction of exciting light beam; P_x, polarizer orientation. Wavelength of exciting light: predominantly the 406- and 436-nm lines of a 100 W mercury lamp, intensity $\approx 5 \times 10^3$ erg cm^{-2} s^{-1}. CP, *Chlorella pyrenoidosa* (no. 395), Sc, *Scenedesmus obliquus*, Sp, fresh spinach chloroplasts, CV, *Chlorella vulgaris*, Ph, *Phormidium luridum*. (From 1972. N. E. Geacintov et al. *Biochim. Biophys. Acta.* **267**:65–79; reproduced with permission of the authors and publishers).

Geacintov et al. (1) suggested a model in which whole *Chlorella* cells are oriented by the field because of an anisotropy in the diamagnetism of some of the cell components and in which the pigment molecules must possess an overall preferential alignment with respect to the cell. Orientation of individual pigment molecules by the field was ruled out for the following reasons. First, the field dependence occurs at such low fields that the anisotropy in the diamagnetic susceptibility of the oriented object should be of the order of magnitude of 10 cm^3 mol^{-1}, whereas for organic molecules the susceptibility itself is in the range of 10^{-4}–10^{-6} cm^3 mol^{-1}. Indeed, no fluorescence polarization was observed in benzene solutions of chlorophyll *a* in fields of up to 100 kG, indicating that if the chlorophylls are the molecules responsible for the orientation, cooperation of a larger number of rigidly connected molecules is required. Secondly, the cell diameter, calculated from the experimental results for the viscosity dependence of the relaxation time of the magnetic field effects, agreed approximately with the observed diameter of a *Chlorella* cell.

By staining with a dye, rhodamine B, known to become oriented with its transition vector preferentially parallel to the lamellar plane (18), it was concluded (14) that the lamellar plane is preferentially oriented perpendicular to the field. Since the transition moments of the chlorophylls were found also to have larger components perpendicular to the field, this meant that in the cells the chlorophylls oriented in such a way that the transition dipoles were preferentially parallel to the lamellar plane. Orientation of membranes perpendicular to a magnetic field is now seen rather generally (10–12).

In early considerations (13), the chlorophylls were thought to be candidates for the dominant anisotropic species, because the lipid contributions could be ruled out on energetic considerations. The proteins were assumed fairly isotropic. However, it now appears that either the protein aromatic residues (16, 19) or the peptide bonds in the α-helices (12, 20), or both, can contribute sufficient anisotropy for magnetic orientation. In this paper we describe and report the results of a calculation applicable to axially symmetric systems in which the optical and diamagnetic species may be taken as either identical or distinct.

D. Summary of Procedures

(*a*) We first set up a theoretical framework for describing the distribution of lamellar segments based on assumed axial symmetry. This enables us to handle not only platelets, cylinders, and cup and cap shapes, but also a generalized cylindrical distribution such as might be inferred from a cross section in an electron micrograph. (*b*) We then consider the lamellae of the model structure to be populated with diamagnetically anisotropic (e.g., chlorophyll) molecules whose orientations are partially specified. For the case of planar aromatics, the normal **u** to the plane of the ring is assumed to make an angle α with the normal to the lamellar plane, but the molecule is otherwise randomly oriented. The angle α may also represent the angle between the membrane normal and the molecular axis about which the largest diamagnetic component exists in *any* species taken to dominate the magnetic energy, not necessarily planar aromatics. At this stage, it is possible to calculate the magnetic energy of the chloroplast when

the axis of symmetry makes an angle θ with an external magnetic field (c) To the previously given geometry we add the specification that the transition moment of the Q_y absorption/emission band is oriented at an angle θ_y with respect to the normal to the lamellar plane. Because the transition moment lies in the plane of the porphyrin ring, θ_y must lie between $(\pi/2) - \alpha$ and $\pi/2$ if the optical and diamagnetic effects arise from the same species. At this stage it is possible to calculate the relative intensities of emissions of various polarizations with respect to the magnetic field or the axis of symmetry. (d) Using the magnetic energy from stage (b) and a Boltzmann factor, the optical intensities computed in stage (c) may be thermally averaged to predict the magnetic-field and temperature dependence of the emission polarization.

II. DESCRIPTION OF MEMBRANE DISTRIBUTIONS

A. Shape Parameter for Cylindrical Distributions

All physical quantities ultimately important to this calculation depend on the orientations of membrane surfaces with respect to some reference axis such as the direction of an applied magnetic field (Fig. 2). Because of the assumed cylindrical symmetry of the surfaces about a symmetry axis (SA), intermediate stages of the calculation involve certain averages over the distribution of membrane orientations around the SA. It is therefore useful first to focus attention on the SA-membrane system.

As illustrated in Fig. 2a, the normal to a membrane is denoted by the unit vector **n** at spherical coordinates θ, ϕ (not shown) with respect to the SA. A cylindrical surface about the SA can be characterized by an area distribution $A(\theta)$, so that $dA = 2\pi r_\perp ds = A(\theta)d\theta$ is the contribution to the total surface area by an annular segment of width ds at a distance $r_\perp$ from (and measured perpendicular to) the SA. (For an arbitrary surface, there may be two or more disconnected regions contributing to $A(\theta)$ at the same θ and having values of $r_\perp$ which may or may not be the same.) In the perfect sphere of radius R, for example, there is a simple analytical relation between ds and $d\theta$, and we have $dA = 2\pi R^2 \sin\theta d\theta$. The distribution in any even is such that $\int_0^\pi A(\theta)d\theta$ is the total surface area.

In computing the diamagnetic anisotropy energy and emission polarizations in later sections of this paper, it is found that the following very simple average occurs frequently:

$$b = Av(\cos^2\theta) = \frac{\int_0^\pi A(\theta)\cos^2\theta d\theta}{\int_0^\pi A(\theta)d\theta}. \qquad (1)$$

This average turns out to be a useful shape parameter. Its value is 1 for a flat disk, 0 for a right circular cylinder, and $\frac{1}{3}$ for a sphere or hemisphere. At the ends of the b scale, therefore, it is possible to regard distributions as "cylinderlike" ($b \approx 0$) or "disklike" ($b \approx 1$). Fig. 3 displays the shape parameters for several common forms.

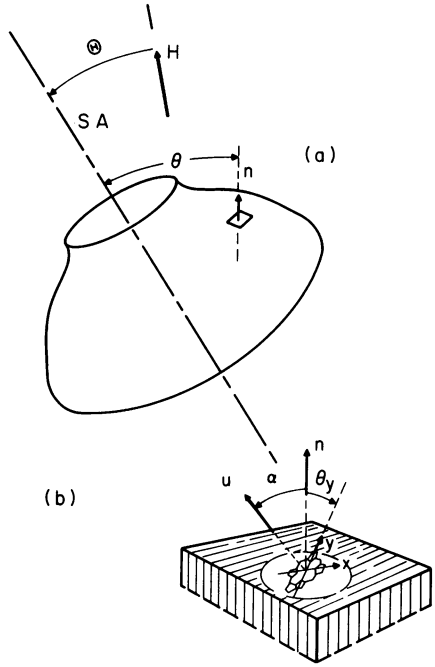

FIGURE 2

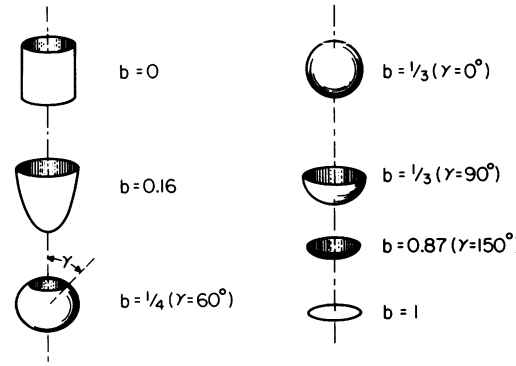

FIGURE 3

FIGURE 2 (a) Relationships among the direction of the magnetic field (**H**), cell symmetry axis (SA), and unit normal to a segment of a membrane (**n**). (*b*) Relationships among **n**, the unit normal to the plane of a chlorophyll molecule (**u**), and the transition dipole moment for the Q_y band (**y**). The unit vector **y** is at polar angle θ_y with respect to **n**. *b* may also refer to a molecule of purely diamagnetic interest, in which case the molecular framework represents a plane in which the principal diamagnetic currents are induced, and *u* the axis carrying the largest (in absolute magnitude) diamagnetic tensor components. Although not shown explicitly, θ_x is defined for the molecular *x* axis in the same way as θ_y.

FIGURE 3 Shape parameters for several forms. The quantity *b* is defined in Eq. 1 and represents the average of the square of the direction cosine of the surface normal over the entire surface in a coordinate system in which the SA (dotted line) lies at $\theta = 0$. The paraboloid illustrated has a height-radius ratio of 3/2. For the truncated sphere with opening angle γ, one has in general $b = (1 + \cos^3\gamma)/[3(1 + \cos\gamma)]$. In order of increasing *b*, these shapes are referred to as cylinder, paraboloid, cup, sphere, hemisphere, cap, and disk.

The progression from cylinder to plate is seen to be rather continuous. The truncated sphere is special in that *b* cannot lie below $\frac{1}{4}$.

B. Example: Analysis of Electron Micrographs

Two examples of the "cup-shaped" *Chlorella* cell are shown in Figs. 4 and 5. These electron micrographs were prepared by Park (21 and private communication) from the Emerson strain of *C. pyrenoidosa*. The SAs shown are rather arbitrarily positioned. For obvious reasons any characterization of the lamellae as cylindrically symmetric about any axis would be very crude. Nevertheless, such a model is preferable to as-

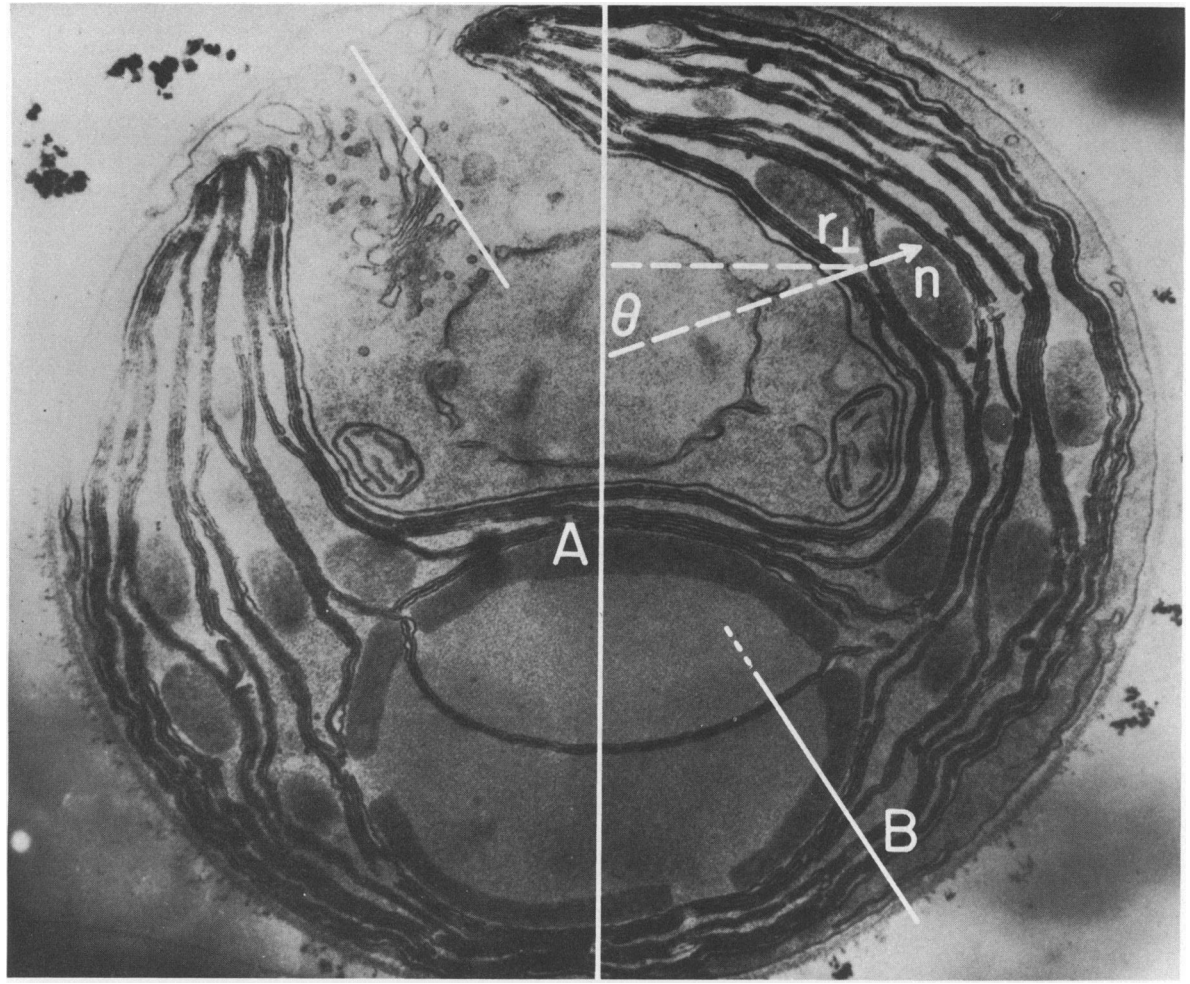

FIGURE 4 Electron micrograph of a cross section of *Chlorella pyrenoidosa* (after Park [21]). The heavy line is the assumed SA (A), and a typical normal vector (**n**) is shown along with the perpendicular distance to the axis ($r_\perp$). Axis B, not used in the calculation, is an alternative shown for comparison. The underlying photograph is reproduced with permission of Academic Press, Inc., and R. B. Park. (×55,000)

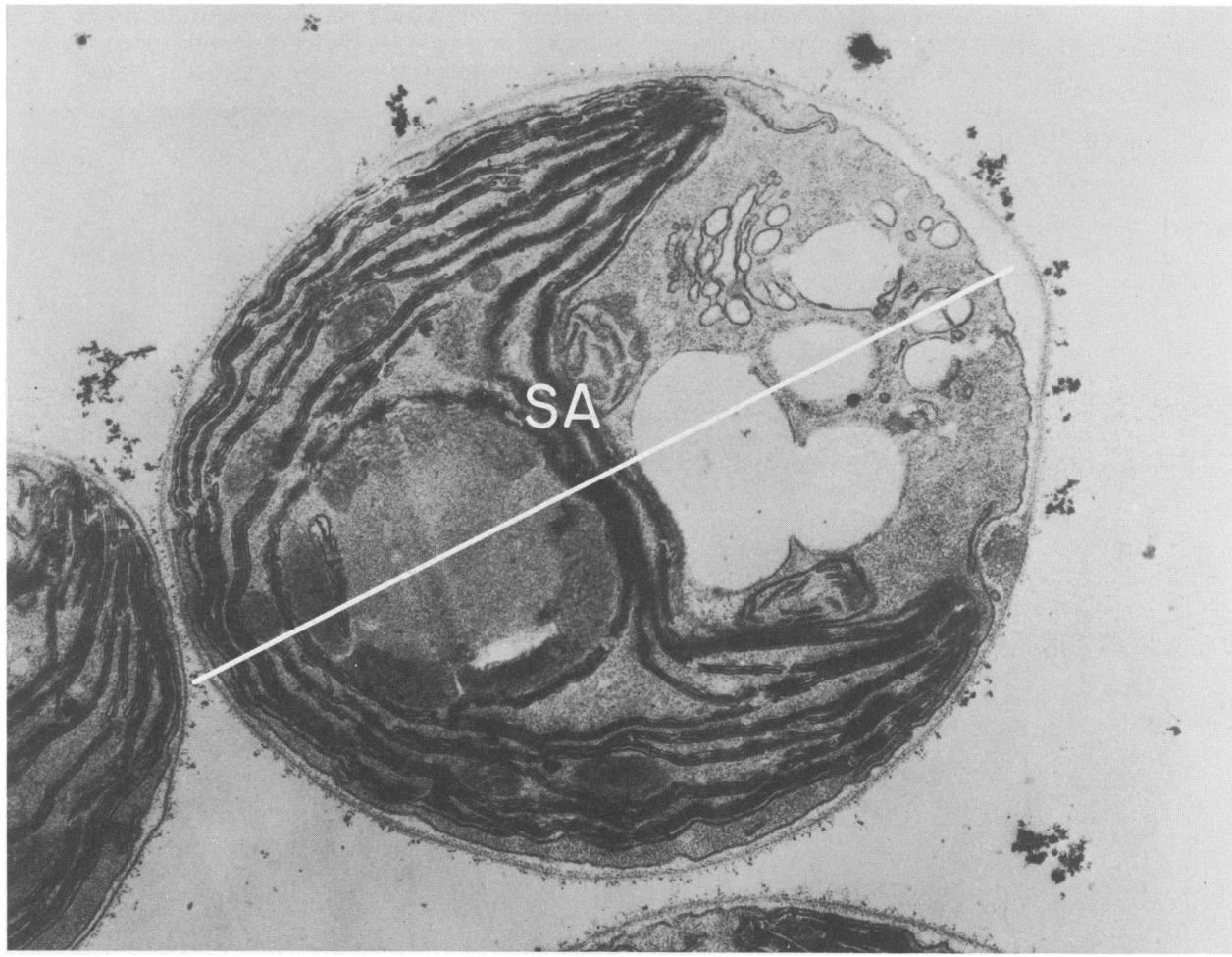

FIGURE 5 Electron micrograph of a cross section of *Chlorella pyrenoidosa* (R. B. Park, private communication). For details, see caption of Fig. 4. (×38,000).

suming flat membranes or adopting an arbitrary cup shape. The latter would introduce an unmanageable number of parameters.

Normals to the lamellae were constructed and the angular distribution of these normals, with a 5° resolution, were calculated directly from the micrographs. For a segment of length Δs, the assumed total area of lamellar material is given by $n \cdot 2\pi r_\perp \Delta s$, where $r_\perp$ is the distance to the SA along a line perpendicular to that axis, and n is the number of layers of dark material associated with the segment under consideration. We define $A(\theta)\Delta\theta$ as the total effective area having normals between $\theta - (\Delta\theta/2)$ and $\theta + (\Delta\theta/2)$. Fig. 6 shows the angular distribution calculated from the lamella of the left half of Fig. 4, excluding the tip to the left of axis A at the top. Clearly the cell is not cylindrically symmetrical about axis A, but neither is it symmetrical about axis B, wherein the right half topologically resembles the left half of the axis A case.

That our numerical results are not unreasonable can be seen as follows. The integrated effective lamellar area

$$A = \sum_\theta A(\theta)\Delta\theta,$$

from Fig. 6, is 1.03×10^{-5} cm^2. As there are about 3×10^8 chlorophyll molecules per *Chlorella,*[1] the implied area density of chlorophyll molecules is 1/340 Å^2. Because the internal membranes are 5–10% chlorophyll by weight (23), the effective individual chlorophyll molecule area is 20–40 Å^2, a reasonable value.

The shape parameter for the cell of Fig. 4 is $b = 0.249$, slightly less than that of the ideal $\gamma = 60°$ spherical cup. From a similar distribution computed for the cell of Fig. 5, we obtain $b = 0.150$, similar to that of the simple paraboloid.

III. THERMAL DISTRIBUTION OF ORIENTED MEMBRANES

A. Diamagnetic Anisotropy Energy

Our calculation will be based on the assumption that a nonrandom distribution of some molecular species, locked together on the membranes, is responsible for the overall diamagnetic anisotropy of the cell. As a typical and relevant species we consider the planar aromatics, known to have a diamagnetic susceptibility numerically much greater in the direction normal to the plane of the molecule than in the two directions parallel to it (24). If $\Delta\chi$ is the excess of $\chi_{||}$, the susceptibility component referred to an axis normal to the plane, over $\chi_\perp$, the mean of the two susceptibilities in the plane, the interaction energy of one molecule with the magnetic field H can be

[1] The density of chlorophylls in photosynthetic membranes is about 8×10^{19} cm^{-3}, according to the analysis by Park (reference 21, p. 309). The volume of a spherical shell of radius 2 μm is 3.35×10^{-11} cm^3, and if 10% is membranous, a reasonable estimate because lipid typically comprise 6% of the cell by weight (22), such a cell contains about 3×10^8 chlorophylls.

written (25)

$$W = -\tfrac{1}{2}\Delta\chi H^2 \cos^2\theta'' = -\tfrac{1}{2}\Delta\chi(\mathbf{u}\cdot\mathbf{H})^2 \tag{2}$$

where θ'' is the angle between the field and $\mathbf{u}$, a unit vector in the direction of largest susceptibility as described above. We have omitted the contribution to W which is independent of $\mathbf{H}$. If there are $n_i(\mathbf{u})$ molecules of type i, per unit solid angle, each having anisotropic susceptibility $\Delta\chi_i$, the anisotropic part of the energy due to the entire distribution of molecules will be

$$W = \sum_i \int d\mathbf{u} n_i(\mathbf{u}) \left[-\frac{1}{2}\Delta\chi_i(\mathbf{u}\cdot\mathbf{H})^2\right]. \tag{3}$$

Here $d\mathbf{u} \equiv \sin\theta_u d\theta_u d\phi_u$, where θ_u, ϕ_u are the angular coordinates of $\mathbf{u}$.

The total anisotropy energy may now be calculated for the assumed cylindrically symmetric distributions developed above. We stipulate that the axes of greatest molecular susceptibility make an angle α with respect to the normal to the membrane (see Fig. 2*b*) but are otherwise randomly distributed. For N diamagnetic molecules of a single ($\Delta\chi_i = -|\Delta\chi|$), W is then averaged over the azimuthal angles of $\mathbf{u}$

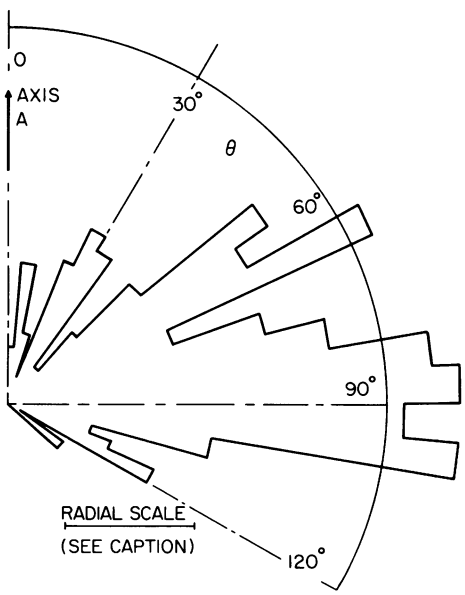

FIGURE 6

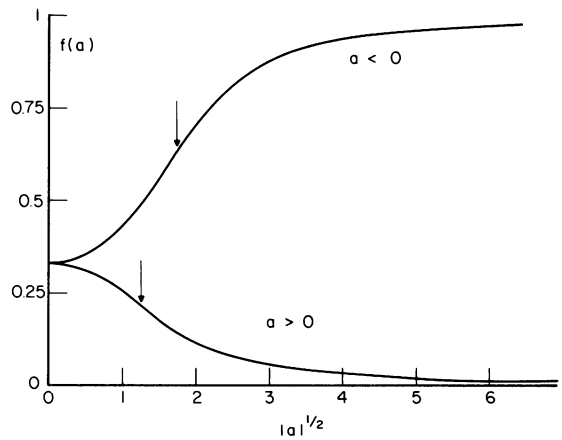

FIGURE 7

FIGURE 6 Angular distribution $A(\theta)$ of the normals to the lamellar planes in Fig. 4 with cylindrical symmetry assumed. For the definition of $A(\theta)$, see text. The scale segment corresponds to an effective area density of 2.5×10^{-7} cm^2 per 5° segment.

FIGURE 7 The function $f(a)$ (see Eqs. B1, B4, and B5) as a function of $|a|^{1/2}$. The upper curve is appropriate for negative values of a, the lower for positive values. Arrows mark the inflection points.

and **n**, with the result (see Appendix A)

$$W(\Theta) = \tfrac{1}{8} |\Delta\chi| H^2 N[1 + b + (1 - 3b)\cos^2\alpha + (1 - 3b)(1 - 3\cos^2\alpha)\cos^2\Theta], \tag{4}$$

where b is the shape parameter discussed in section II. For the special angle $\alpha = \cos^{-1}\sqrt{1/3}$ the anisotropy has no effect on the Θ dependence of the magnetic energy, and on either side of this special angle Θ dependence has opposite signs. Similar remarks hold for the shape parameter: if $b = \frac{1}{3}$ the Θ dependence vanishes, and it has opposite signs on the two sides of this condition. The overall sign of the coefficient of $\cos^2\Theta$ is crucial to the orientational behavior of the cell, as will be seen in the next section.

The essential parameters in Eq. 4 are now α, Θ, H, and $N|\Delta\chi|$. Of these only α and $N|\Delta\chi|$ are "free," because Θ will participate in a Boltzmann average or otherwise determine the equilibrium orientation, and H is the principal experimental variable. Moreover, $N|\Delta\chi|$ is involved only in determining the inflection point of the experimental curves as a function of H, not in saturation (large H) limits. Most of our analysis refers to saturation values, so a single free parameter (α) effectively remains in the model at this stage for a given cylindrical membrane distribution.

B. Boltzmann Averages

The magnetic field establishes a reference direction for the optical measurements described in the next section. Quantities $F(\Theta, \Phi)$ which depend on the orientation of the SA with respect to the field will, in practice, be measured at thermal equilibrium, so the following average must be computed:

$$\langle F \rangle = \frac{\int_0^{2\pi} d\Phi \int_0^{\pi} \sin\Theta d\Theta F(\Theta,\Phi) e^{-W(\Theta)/k_B T}}{2\pi \int_0^{\pi} \sin\Theta d\Theta e^{-W(\Theta)/k_B T}}, \tag{5}$$

where W is the energy of the system calculated above, k_B is Boltzmann's constant, T is the absolute temperature, and Φ is the azimuthal angle (not shown in Fig. 2*a*). In an angular average of this type, all terms in the energy independent of angles contribute factors that cancel, and inasmuch as W is independent of Φ we obtain

$$\langle F \rangle = \frac{\int_0^{2\pi} d\Phi \int_0^{\pi} \sin\Theta d\Theta F(\Theta,\Phi) e^{-a\cos^2\Theta}}{2\pi \int_0^{\pi} \sin\Theta d\Theta e^{-a\cos^2\Theta}}, \tag{6}$$

where, according to Eq. 4,

$$a = \frac{N|\Delta\chi| H^2 (1 - 3b)(1 - 3\cos^2\alpha)}{k_B T}. \tag{7}$$

As we will see below, the sign of a is central to a quantitative discussion.

The simplest average one may compute is also an important one, namely, the average magnetic energy. That part which depends on Θ averages to

$$\begin{aligned} <W> &= \frac{N}{8} \mid \Delta\chi \mid H^2(1 - 3b)(1 - 3\cos^2\alpha)<\cos^2\Theta>, \\ &= k_B T \cdot a \cdot \left(\int_0^1 y^2 e^{-ay^2} dy \Big/ \int_0^1 e^{-ay^2} dy \right), \\ &= k_B T \cdot a \cdot f(a), \end{aligned} \tag{8}$$

where the function $f(a)$ has the form shown in Fig. 7, plotted as a function of $\mid a \mid^{1/2}$. The form depends crucially on the sign of a. (Mathematical details are found in Appendix A.) At small magnetic fields or high temperatures, the limiting value of $<W>$, with the Θ-independent terms of Eq. 4 reincluded, becomes $\mid \Delta\chi \mid H^2 N/6$, regardless of the sign of a. Consider again the variable part (8) but at high fields or low temperatures. Eqs. A6 and A7 yield

$$<W> \rightarrow \tfrac{1}{2} k_B T \qquad (a \rightarrow +\infty)$$

and

$$<W> \rightarrow -CH^2 \qquad (a \rightarrow -\infty),$$

where C is a positive constant. Physically, the case $a > 0$ corresponds to a geometry in which the Θ-dependent part of the magnetic energy is minimized at values of $\Theta = 90°$, whereas the case $a < 0$ corresponds to one in which it is minimized at $\Theta = 0$ or $180°$. In the former case, because the variable part of the magnetic energy is zero at 90°, the leading term in the average energy is just the thermal energy associated with the Θ degree of freedom. In the latter case, the Boltzmann average allows the field-dependent part to dominate.

C. Implications for Orientation

The magnetic energy calculation shows clearly how the orientation of cylindrical membrane systems is determined by two factors: the shape parameter b determines the sign of $(1 - 3b)$ and the molecular tilt angle determines the sign of $(1 - 3\cos^2\alpha)$. Together these factors determine the sign of a. Referring to Fig. 3 and to the end of the previous paragraph, we reach the following conclusions.

COS$^2\alpha > \frac{1}{3}$: THE PLANES OF THE PRINCIPAL DIAMAGNETIC CURRENT LOOPS ARE MORE NEARLY PARALLEL TO THE MEMBRANE SURFACE The sign of a here is the sign of $(3b - 1)$. Therefore the cylinder, paraboloid, and 60°-cup shapes will tend to align with the SA parallel to the magnetic field. The cap and disk will align parallel to the field, i.e., with the SA perpendicular to it. The sphere and hemisphere do not orient.

COS$^2\alpha < \frac{1}{3}$: THE PLANES OF THE PRINCIPAL DIAMAGNETIC CURRENT LOOPS ARE MORE NEARLY PERPENDICULAR TO THE MEMBRANE SURFACE The sign of a here is the sign of $(1 - 3b)$. Therefore, the cylinder, paraboloid, and 60°-cup shapes will tend to align with the SA perpendicular to the field. The cap and disk will align perpendicular to the field, i.e., with the SA parallel to it. The sphere and hemisphere do not orient.

D. *Implications for Anisotropic Diamagnetic Species*

If, as has frequently been assumed, the chromophores themselves are the diamagnetically important species, the inflection points of $f(a)$ (Fig. 7) are directly comparable to those appearing in the optical data of Fig. 1. As we will see in the next section, this is true because it is again averages of $\cos^2\Theta$ that determine the magnetic-field dependence of the optical data. To test this possibility in the case of chlorophyll, a value of $\Delta\chi$ must be estimated. Two approaches are possible. On the Platt ring model (26) a first-order calculation of the diamagnetic energy is straightforward and yields

$$\chi_{\parallel} = -9e^2r_0^2/4\,mc^2 \tag{9a}$$

$$\chi_{\perp} = -9e^2r_0^2/8\,mc^2 \tag{9b}$$

or

$$|\Delta\chi| = 9e^2r_0^2/8\,mc^2, \tag{10}$$

where r_0 is the ring radius, e the electronic charge, m the electron mass, and c the velocity of light. For a ring radius of 3.3 $\mathring{A}$, which crudely approximates the pi-electron system of the chlorophylls, $|\Delta\chi| = 208 \times 10^{-6}\text{cm}^3\text{mol}^{-1}$. The other method available is Pascal's (27), in which the distinction between $\chi_{\parallel}$ and $\chi_{\perp}$ is not so clear, but which yields the same order of magnitude for the individual components of χ. We take a simple sum of Pascal's partial susceptibilities for $\chi_{\perp}$, obtaining -265×10^{-6} $\text{cm}^3\text{mol}^{-1}$, and add his corrections for bonds and ring sharing to characterize $\chi_{\parallel}$, obtaining -288×10^{-6} $\text{cm}^3\text{mol}^{-1}$. Clearly $\Delta\chi$ is too small here, and we tend to trust the Platt model value of because it is based more solidly on the planar geometry of the system. The orders of magnitude obtained from the two methods agree, and Platt's compares reasonably with related planar aromatic molecule values. For example, $|\Delta\chi|$ s in benzene, phenanthrene, and phthalocyanine are 62, 166, 380 $\times$ 10^{-6} cm^3 mol^{-1}, respectively (24). We adopt the value 208×10^{-6} cm^3 mol^{-1} for chlorophyll *a*.

Let us now compare the experimental curves (Fig. 1) with the general shape expected of magnetic-field dependent quantities (Fig. 7). The average of the two inflection points of $f(\pm|a|)$ can be taken as representative, i.e., $|a|^{1/2} \sim 1.5$ (see Appendix B). Inserting this value into Eq. 7 and defining H_0 as the magnetic field at the inflection point, we obtain the following condition, which may be loosely interpreted as setting the magnetic anisotropy energy per cell equal to the thermal energy in the Θ degree of freedom:

$$\tfrac{1}{36}|N\Delta\chi H_0^2(1 - 3b)(1 - 3\cos^2\alpha)| \sim \tfrac{1}{2}k_BT. \tag{11}$$

Taking $b \sim 0.25$ for the typical cup-shaped cell, the calculated $\Delta\chi$, the observed $H_0 = 5\,\text{kG}$ (16), and $T = 290$ K, we obtain $N|1 - 3\cos^2\alpha| \sim 5.5 \times 10^{-16}$ mole/cell $= 3.3 \times 10^8$ molecules/cell. The quantity N refers to the number of molecules that have the local anisotropy characterized by the angle α. Because, as we argued

above, the typical cell contains about 3×10^8 chlorophyll molecules, it is clear that nearly 100% of the chlorophylls must be included in the anisotropic set. For $b \sim 1$ (disklike membranes), this number is reduced to about 10%. We learn, therefore, that the hypothesis of assigning both optical and diamagnetic behavior to the same molecules carries with it the need to assume a relatively large amount of specific orientation. In the next section we do not make use of the inflection point data and we do allow the two properties to be associated with different species.

IV. FLUORESCENCE INTENSITIES

A. Single Oriented Cell

One of the principal observables in the magnetic orientation experiments mentioned earlier is the dependence on magnetic field of the fluorescence intensity polarized parallel and perpendicular to the field. Inasmuch as we are dealing with the electronically nondegenerate Q_y states of chlorophyll, it is reasonable to assume a simple Lorentz oscillator dipole radiation field, so that the intensities in question are proportional to

$$J_{||} = \sum_i (\mathbf{y}_i \cdot \mathbf{Z})^2 \tag{12}$$

and

$$J_{\perp} = \sum_i (\mathbf{y}_i \cdot \mathbf{X})^2, \tag{13}$$

respectively, where $\mathbf{Z}$ is a unit vector parallel to $\mathbf{H}$, $\mathbf{X}$ is a unit vector perpendicular to $\mathbf{H}$, and $\mathbf{y}_i$ is a unit vector parallel to the Q_y transition moment of molecule i; $\mathbf{y}_i$ is perpendicular to $\mathbf{u}$, the normal to the chlorophyll molecule (see Fig. 2). The sums in $J_{||}$ and $J_{\perp}$ are to be evaluated under the restrictions imposed by the membrane distributions (and by the angle α if the magnetic and optical species are identical). In the absence of such restrictions, both $J_{||}$ and $J_{\perp}$ would have the value $N/3$, where N is the number of molecules in a randomly distributed emitting sample.

Under the assumption that the membrane distribution is cylindrical, and that the azimuthal distribution of normals $\mathbf{n}$ is random, the quantities $J_{||}$ and $J_{\perp}$ are completely specified except for one consideration: the orientation of $\mathbf{y}$ with respect to the membrane surface. We denote its spherical coordinates in the membrane frame of reference by (θ_y, ϕ_y) and observe that θ_y is restricted to the range $(\pi/2) - \alpha_c \leq \theta_y \leq \pi/2$, where α_c is the chromophore tilt angle. There are only two reasonable assumptions about the distribution of $\mathbf{y}$ that lead to tractable results, and we have computed $J_{||}$ and $J_{\perp}$ for each. Assumption *a* is that $\mathbf{y}$ is randomly distributed around the normals $\mathbf{u}$; in other words, in a large sampling of the emitting molecules, there is no correlation between $\mathbf{y}$ and the membrane other than that induced by the molecular tilt angle α_c. In this case, the average projections of $\mathbf{y}$ on the membrane

and perpendicular to it are, respectively,

$$c_{||} = \tfrac{1}{2}(1 + \cos^2\alpha_c), \tag{14a}$$

$$c_{\perp} = \tfrac{1}{2}\sin^2\alpha_c. \tag{14b}$$

Assumption *b* is that **y** is itself tilted at a fixed angle θ_y with respect to the membrane normal. In this case θ_y will enter as a new parameter, because the average projections of **y** on the membrane and perpendicular to it are, respectively,

$$c_{||} = \sin^2\theta_y, \tag{15a}$$

$$c_{\perp} = \cos^2\theta_y. \tag{15b}$$

We now let the cell SA be oriented at (Θ, Φ) with respect to the magnetic field, average over the azimuthal angles of **y**, **u**, and **n**, and over the distribution of normals $A(\theta)$. The results are

$$\frac{J_{||}}{N} = \frac{c_{||}}{4}[1 + b + (1 - 3b)\cos^2\Theta] + \frac{c_{\perp}}{2}[1 - b - (1 - 3b)\cos^2\Theta], \tag{16}$$

and

$$\frac{J_{\perp}}{N} = \frac{c_{\|}}{4}[1 + b + (1 - 3b)\sin^2\Theta\sin^2\Phi] + \frac{c_{\perp}}{2}[1 - b - (1 - 3b)\sin^2\Theta\sin^2\Phi]. \tag{17}$$

(Although the steps leading to Eqs. 16 and 17 are straightforward, they are tedious. For example, the averages in case *a* are complicated by the fact that the appropriate average is to be taken over an angle in the plane of the molecule, not simply over θ_y. Other than this, the necessary procedures are entirely similar to those of Appendix A.)

In the previous section on the magnetic energy we noted that α (molecular tilt) was the only free parameter after averaging for membrane shapes. This is also the case in Eqs. 16 and 17, but in a modified form. Under the random orientation assumption *a*, the quantities $c_{||}$ and $c_{\perp}$ carry an α_c dependence explicitly. Under the θ_y assumption (b), α_c is involved only through the restriction placed on the values of θ_y. If the chromophore is not the diamagnetic molecule, α_c must remain distinct from α. The latter will reappear upon averaging. In case (b) there is no need to consider the chromophore tilt angle, and θ_y assumes the role of the only free parameter in Eqs. 16 and 17. Again, α will reappear upon thermal averaging.

B. Ensemble Average Intensities

Eqs. 16 and 17 must now be averaged over Θ and Φ, using the Boltzmann distribution (Eq. 6). Because there is no Φ dependence in the energy, the Φ average is 1 or

$\langle \sin^2\Phi \rangle = \frac{1}{2}$, and the Θ averages of $\langle \cos^2\Theta \rangle$ are precisely the same as those done in the average energy calculation. We obtain at once (omitting common constant factors)

$$\langle J_{||} \rangle = c_{||}(1 + b) + 2c_{\perp}(1 - b) + (c_{||} - 2c_{\perp})(1 - 3b)f(a) \qquad (18)$$

and

$$2\langle J_{\perp} \rangle = c_{||}(3 - b) + 2c_{\perp}(1 + b) - (c_{||} - 2c_{\perp})(1 - 3b)f(a), \qquad (19)$$

where $f(a)$ is the function previously defined containing the magnetic field, susceptibility, and temperature dependence. In the absence of any orientation ($a \to 0$), the two intensities are predicted to be indistinguishable, as they should be, and as may be seen by substituting $f(a) = f(0) = \frac{1}{3}$ in Eqs. 18 and 19.

Two kinds of predictions may be made from Eqs. 18 and 19. The first involves the dependence of $f(a)$ on magnetic field; the inflection points in these functions may be related to the susceptibilities and anisotropies, as developed earlier in part III. The second kind of prediction, which we choose to discuss in detail because of its insensitivity to the size and origin of the molecular susceptibility, involves the asymptotic values of $\langle J_{||} \rangle$ and $\langle J_{\perp} \rangle$ at large fields. It is known that only modest fields are required to reach saturation (9, 13–16). A convenient single prediction of the theory is the saturation polarization ratio (SPR):

$$\text{SPR} \equiv \left.\frac{\langle J_{\perp} \rangle}{\langle J_{||} \rangle}\right|_{H \to \infty} = \frac{(3 - b)c_{||} + 2(1 + b)c_{\perp} - (1 - 3b)(c_{||} - 2c_{\perp})f(\pm\infty)}{2(1 + b)c_{||} + 4(1 - b)c_{\perp} + 2(1 - 3b)(c_{||} - 2c_{\perp})f(\pm\infty)}. \qquad (20)$$

Because of the crucial dependence of $f(a)$ on the sign of a, the SPR takes on quite different values for positive and negative a; see Eqs. B6 and B7:

$$\text{SPR}(a > 0) = \frac{(3 - b)c_{||} + 2(1 + b)c_{\perp}}{2(1 + b)c_{||} + 4(1 - b)c_{\perp}} \qquad (21)$$

$$\text{SPR}(a < 0) = \frac{(1 + b)c_{||} + 2(1 - b)c_{\perp}}{2(1 - b)c_{||} + 4bc_{\perp}} \qquad (22)$$

At this point we can make a choice of assumptions concerning the orientation of the dipoles on the membrane. Case a, Q_y random in the molecular plane, has been included up to this point for generality. However, upon completing the calculation one finds this case to be uninteresting under almost any circumstance. If the chromophore is identical with the diamagnetic species, case a predicts SPR ≤ 1, which is never observed, and if the species are not identical, case a is either unrealistic or equivalent to case b, depending on the region of α_c. Appendix C includes further details concerning case a. Henceforth we adopt case b as the working model, in which Q_y is fixed

at a polar angle θ_y from the normal to the membrane. We evaluate the corresponding SPR by substituting Eq. 15 in Eqs. 21 and 22:

$$\mathrm{SPR}(a > 0) = \frac{8 + (1 - 3b)(1 - 3\cos^2\theta_y)}{8 - 2(1 - 3b)(1 - 3\cos^2\theta_y)} \tag{23}$$

$$\mathrm{SPR}(a < 0) = \frac{4 - (1 - 3b)(1 - 3\cos^2\theta_y)}{4 + 2(1 - 3b)(1 - 3\cos^2\theta_y)}. \tag{24}$$

A rather definite pattern can be discerned as shown in Fig. 8. Regardless of the size of b, the SPR is greater than unity in only two regions of $\alpha - \theta_y$ space. On the restricted model, in which the chromophore and diamagnetic species are identical, one of these regions shrinks to a triangle, leaving the upper right half as the principal region of interest. The SPR is to be calculated as follows: given b and α, determine the corresponding sign of a. This may be done using Eq. 7 or the notation at the top and bottom of Fig. 8. Accordingly, select Eq. 23 or 24. Alternatively, if the SPR and b are known, Fig. 8 immediately indicates the possible ranges of α and θ_y which are consistent with the theory developed here.

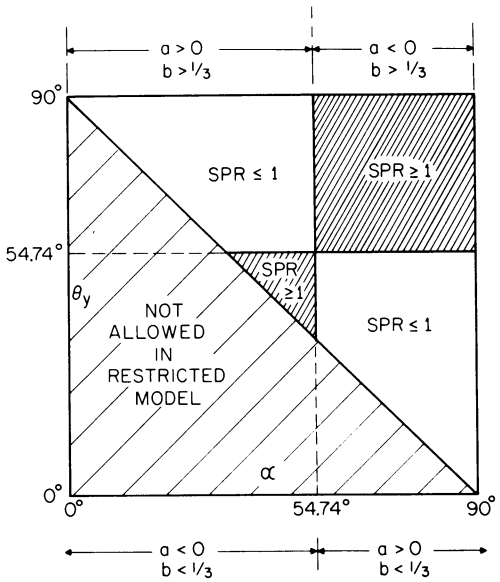

FIGURE 8

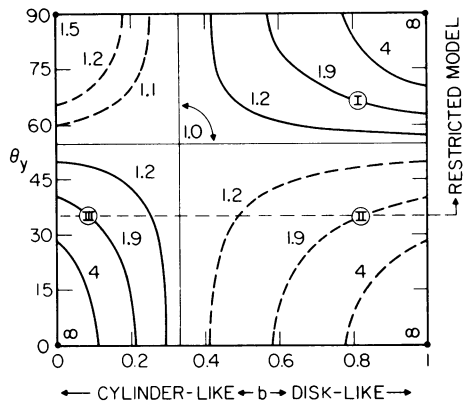

FIGURE 9

FIGURE 8 Ranges of the saturation polarization ratio (SPR) for all possible choices of α, θ_y. In the "restricted" model only the upper right half of this space is available. See text for details. The parameters b and a are the shape parameter and Eq. 7, respectively. In the "unrestricted" model, the disallowed region vanishes, revealing an entire larger square with SPR $\geq$ 1.

FIGURE 9 Lines of constant SPR for cases in which SPR $\geq$ 1. Dashed curves correspond to the case $a > 0$, and solid lines to the case $a < 0$. Roman numerals I, II, III locate the three regions of SPR ~ 1.9 discussed in the text. The region below $\theta_y = 35.26°$ is unavailable in the restricted model.

The vertical and horizontal lines at 54.74° are of some interest. For $\theta_y = 54.74°$ it is clear that both Eqs. 23 and 24 predict SPR = 1. For $\alpha = 54.74°$, SPR is *formally* 1, but for the reason that $a = 0$, and "saturation" is a misnomer. Therefore, except at $\theta_y = 54.74°$, a discontinuity in SPR is expected as α crosses 54.74°.

C. Comparison with Experiment

In his study of the fluorescence of various cells in magnetic fields, Becker (16) found that the SPR was generally in the range of 1.2–1.9, the latter value belonging to *Chlorella.* Typical values are 1.5–1.6, and none are below 1.0. For those organisms whose membrane systems consist generally of parallel planes, such as spinach chloroplasts, and for those situations in which membrane fragments can be taken as flat, the geometrical factor b is equal to or near unity. From our results, Fig. 8, and the experimental fact that SPR > 1, we can conclude that α and θ_y are both on the same side of the "magic angle" 54.74°. Furthermore, if the chromophore is the dominant magnetic species, the most probable situation is that both α_c and θ_y are greater than the magic angle. Even this restricted case is consistent with the data to be quoted below. However, *Chlorella,* the organism that inspired the present study, is apparently anomalous, as we shall now argue.

If we adopt 1.9 as the actual value of SPR for *Chlorella,* we may further restrict the class of membrane geometries that are consistent with the hypotheses being tested. For this purpose we map out lines of constant SPR in $b - \theta_y$ space, as shown in Fig. 9. The curves in this space corresponding to SPR = 1.9 are found at the upper right (case I), the lower right (case II), and the lower left (case III). Cases II and III correspond to the lower left part of Fig. 8, case I corresponds to a portion of the upper right square. Although we shall discuss implications for the specific case of SPR = 1.9, it should be clear from Fig. 9 that different values can be analyzed in a similar way, with stronger conclusions if SPR > 1.9 and weaker conclusions if SPR < 1.9.

Table I summarizes the implications of Fig. 9. For each case the predictions of both the unrestricted model and the restricted model are shown, and in case III a separate column is devoted to the special case in which one *Chlorella* micrograph (Fig. 5) can actually accommodate an SPR of 1.9. The message contained in Table I is that a major reassessment of some aspect of our understanding of *Chlorella* orientation is necessary. In cases I and II the predicted disklike shape is not that commonly associated with *Chlorella.* In cases II and III the orientation of the membranes with respect to the field is not that which has always been observed (perpendicular) (10–12). In cases II and III, moreover, the required θ_y disagrees with linear dichroism data which show that $\theta_y \approx 61$–64° (Breton et al. [17]; Becker [16]); similarly, the limits on θ_x agree only tenuously with similar measurements by the same authors ($\theta_x \lesssim 55°$), and certainly disagree on the restricted model. (The linear dichroism data are not, however, in conflict with case I.) Taking another approach, we may quote the careful analysis of Paillotin and Breton (28), who deduced the wavelength dependence of the orientation of absorption oscillators from linear dichroism and electrochromism data on spinach chloroplasts. They found that the longest wavelength oscillators were oriented with Φ (our θ_y) at least as large as 73°. Although a different organism is involved

TABLE I

COMPARATIVE PREDICTIONS OF THE THEORY AS APPLIED TO CASES I, II, AND III OF Fig. 9

	Case I		Case II		Case III		
	Unrestricted model	Restricted model	Unrestricted model	Restricted model	Unrestricted model	Restricted model	Unrestricted, special case
Shape	Nearly disk, with $0.58 \leq b \leq 1$			Disk, $0.82 \leq b \leq 1$	Nearly cylinder, $0 \leq b \leq 0.21$	Cylinder, $0 \leq b \leq 0.08$	$b = 0.15$
a, α	$a < 0, \alpha > 55°$		$a > 0, \alpha < 55°$		$a < 0, \alpha \leq 55°$		
Implied orientation	SA $\parallel$ to field, disk surfaces $\perp$ to field		SA $\perp$ to field, disk surfaces $\parallel$ to field		SA $\parallel$ to field, surfaces of cylinder $\parallel$ to field		
Q_y dipole tilt	$63° \leq \theta_y \leq 90°$		$0 \leq \theta_y \leq 40°$	$35.3° \leq \theta_y \leq 40°$	$0 \leq \theta_y \leq 40°$	$35.3° < \theta_y \leq 40°$	$\theta_y = 28°$
Chromophore tilt α_c	$90° - \theta_y \leq \alpha_c \leq 90°$	Same as unrestricted case, plus $\alpha_c > 55°$	$50° \leq \alpha_c \leq 90°$	$50° \leq \alpha_c \leq 55°$	$50° \leq \alpha_c \leq 90°$	$50° \leq \alpha_c \leq 55°$	$62° \leq \alpha_c \leq 90°$
Q_x dipole tilt	θ_x arbitrary; $\theta_y \geq 27°$ if $\theta_y = 63°$	$\theta_x \leq 47°$; $27° \leq \theta_x \leq 47°$ if $\theta_y = 63°$	$50° \leq \theta_x \leq 90°$	$\theta_x \approx 90°$ only	$50° \leq \theta_x \leq 90°$	$\theta_x \approx 90°$ only	$62° \leq \theta_x \leq 90°$

All symbols are those used in the text, e.g., a is the exponent parameter (Eq. 7), α is the tilt angle of the principal diamagnetic axis of the orienting species, and b is the shape parameter. In the "unrestricted model," the chromophore tilt angle α_c is not necessarily the same as α, but in the "restricted model" the two are identical.

here, this result can be considered supportive of case I, in view of the universality of many aspects of green plant photosynthesis.

Becker's own analysis of the *Chlorella* data may be viewed in the context of Fig. 9 as follows. Not having a full geometric calculation, he calculated an average θ_y of about 62° referred to a plane perpendicular to the field, which corresponds to the point $b = 1$, $\theta_y = 62.8°$ (on the case I curve). He noted that this approximation should be suppressing the SPR, so that 1.9 was to be regarded as a minimum value; this idea is confirmed by our trend of SPR as b changes. Suppose, for example, that the measurement of 1.9 corresponded to $b = 0.65$ and $\theta_y = 75°$. Then the SPR would increase as b is increased, keeping θ_y fixed. Becker further noted that $\theta_y = 62°$ was a minimum value, which is also confirmed by our diagram. His remarks about "minima" are to be read "a lower limit, appropriate to the case in which the membranes are, in fact, flat."

The calculated geometrical factors for *Chlorella* ($b = 0.249$ and 0.150) are compatible with *none* of the allowed regions in $b - \theta_y$ space for SPR = 1.9 in the restricted model, but as noted in the last column of Table I the unrestricted model holds for $b = 0.15$ in case III, carrying with it all the difficulties just outlined. Therefore the presently available *Chlorella* fluorescence polarization data in a saturating magnetic field cannot be understood on the basis of a straightforward model calculation if the membrane structure of *Chlorella* is typified by the cuplike structures of Figs. 4 and 5. We now examine the principal assumptions underlying this conclusion. They fall into two main categories relating to molecular distribution on the membranes and overall geometry of the membrane.

The primary assumptions about molecular distribution we have made here are: that there is on average azimuthal symmetry about the normals to the membrane, and that the tilt angles θ_y, α, and α_c are precise. To remove the azimuthal symmetry would require an enormously detailed model outside the bounds of reason at this point. To place distributions on θ_y might change the SPR slightly, as may be seen by performing a visual average in Fig. 9 (with a sin θ_y weight factor in mind) but the unique place of α in the theory as a determinant of the sign of a would be little affected. Its average value would assume that role.

The membrane geometry assumptions are of two kinds: structural and dynamic. Although most micrographs of *Chlorella* show cuplike cross sections, it is not ruled out that the structure actually has a folded-sandwich character (i.e., resembles a short frankfurter roll). This seems to us the only way to reconcile the micrographs with case I. Dynamically, we are assuming that the main membrane structure is not distorted by the field itself. A view consistent with the micrographs and the SPR data would be that the membranes are actually distorted by the field in such a way that the structure parameter b is pushed from 0.15 or 0.25 to a value >0.58. However, this is a drastic hypothesis because there should be a much larger effect seen in the decay of the polarization after the magnetic field is switched off. The only remaining possibility seems to be rearrangement of chlorophyll protein complexes or of other diamagnetically anisotropic constituents sufficient to alter the *local* geometry. This, too, is drastic because the amount of anisotropy energy is actually very small.

V. CONCLUDING REMARKS

A theory of fluorescence emission as affected by magnetic orientation, designed to accommodate a range of axial membrane geometries, has been shown to be consistent with most available data. One anomaly appears to be the case of *Chlorella.* Further work that might unravel the puzzle could include freezing magnetically oriented cells, followed by electron microscopy to determine whether major membrane distortion is occurring. On the theoretical side, additional information may be extracted from fluorescence polarization studies (in the usual sense, wherein the memory of the excitation polarization is measured). A detailed theory without considerations of magnetic orientation has been presented by Michel-Villaz (29). Here, however, the extent of energy transfer is an important consideration and the existing transfer appears to wash out most of the memory. Perhaps a full extension of the formalism of this paper to the absorption and linear dichroism data would be more fruitful. In the part that such data play in ruling out cases II and III, we have implicitly assumed that they have been analyzed in a way consistent with our model. Another refinement in the model would be the inclusion of some of the known correlations between transition dipole orientations in light-harvesting chlorophyll-protein complexes deduced recently (30) from data on fluorescence polarization.

The authors are indebted to Prof. N. E. Geacintov and Dr. J. F. Becker for stimulating discussions, to Prof. R. B. Park for supplying originals of his *Chlorella* micrographs, and to Mr. M. Ohya for molecular susceptibility calculations.

This work was supported in part by the National Science Foundation under grants PCM-75-19638 and PCM-77-20230. Dr. Davidovich was supported in part by the Brazilian agency Conselho Nacional de Pesquisas.

Received for publication 18 May 1978.

APPENDIX A

The average leading to Eq. 4 proceeds most easily through the introduction of an auxiliary angle θ', the polar angle of **H** as viewed from **n**. Holding **H** and **n** fixed and averaging over all orientations of **u** about **n**, we obtain

$$<\cos^2(\mathbf{u},\mathbf{H})>_{\phi_u} = \tfrac{1}{2}[(1 - \cos^2\alpha) + \cos^2\theta'(3\cos^2\alpha - 1)], \qquad (A1)$$

where $<\cdots>_{\phi_u}$ indicates an average over azimuthal angles of **u** in the frame of reference in which **n** lies along the polar axis ($\theta_u = \alpha$). Next, $\cos\theta'$ is expressed in terms of Θ, Φ, θ, and ϕ, where θ and ϕ are the polar and azimuthal angles of **n** in the frame of reference in which the SA is the polar axis. The result, averaged over the azimuthal angle, is

$$<\cos^2\theta'>_{\phi} = \tfrac{1}{2}[(1 - \cos^2\theta) + \cos^2\Theta(3\cos^2\theta - 1)]. \qquad (A2)$$

The further average of Eq. A1 over ϕ is therefore

$$<\cos^2(\mathbf{u},\mathbf{H})>_{\phi,\phi_u} = \tfrac{1}{4}[(1 + \cos^2\theta) + (1 - 3\cos^2\theta)\cos^2\alpha + (1 - 3\cos^2\theta)(1 - 3\cos^2\alpha)\cos^2\Theta]. \qquad (A3)$$

Finally, the weighting in θ over the membrane distribution converts $\cos^2\theta$ everywhere in this equation to b, resulting in Eq. 4 when the overall average is inserted in Eq. 3.

APPENDIX B

The thermal averaging carried out in sections IV and V involves the function

$$f(a) = \frac{\int_0^1 y^2 e^{-ay^2} dy}{\int_0^1 e^{-ay^2} dy}. \tag{B1}$$

Here a may take on any real value. In our application it is proportional to the square of the applied magnetic field and inversely proportional to the temperature (see Eq. 7). The nature of the integrals in $f(a)$ depends heavily on the sign of a. Let us introduce the following standard functions (31) known as the error function and Dawson's integral, respectively:

$$erf x = 2\pi^{-1/2} \int_0^x e^{-t^2} dt \tag{B2}$$

$$F(x) = e^{-x^2} \int_0^x e^{t^2} dt. \tag{B3}$$

When $a \geq 0$, the denominator of $f(a)$ is $(\pi/4a)^{1/2} erf a^{1/2}$ and when $a \leq 0$ it is $b^{-1/2} e^b F(b^{1/2})$, where $b \equiv -a \geq 0$. Integration of the numerator by parts and further simplification leads, for a positive, to

$$f(a) = (2a)^{-1}[1 - (2/\pi)^{1/2} e^{-a} (erf a^{1/2})^{-1}] \tag{B4}$$

and, with a negative and b positive,

$$f(-b) = (2b)^{-1}\{b^{1/2}[F(b^{1/2})]^{-1} - 1\}. \tag{B5}$$

The limiting forms of $f(a)$ may be worked out using the known asymptotic forms of the functions B2 and B3, with the following results:

$$f(a) \to 0 + 1/2a + 0(1/a^2) \quad (a \to +\infty) \tag{B6}$$

$$f(-b) \to 1 - 1/2b + 0(1/b^2) \quad (b \to +\infty) \tag{B7}$$

$$f(a) \to \tfrac{1}{3} - \tfrac{7}{90} a + 0(a^2) \quad (a \to 0+) \tag{B8}$$

$$f(-b) \to \tfrac{1}{3} + \tfrac{4}{45} b + 0(b^2) \quad (b \to 0+). \tag{B9}$$

The different behaviors of f at large positive and negative arguments reflect the weighting induced by the exponential, as seen in Eq. B1. With positive a, the values of y^2 near 0 dominate, whereas with negative a, values of y^2 near 1 dominate.

The inflection points of the function $f(a)$, as well as its limiting values, depend on the sign of a. By maximizing the first derivative of Eqs. B4 and B5, we have found that the inflection points occur at $a^{1/2} = 1.25$ and $b^{1/2} = 1.74$. The functions themselves are shown in Fig. 7.

APPENDIX C

To elaborate on the molecular orientation assumption case a (see section IV), we substitute Eq. 14 in Eqs. 21 and 22. The result, after considerable rearrangement, is a pair of expressions

for the SPR which depend on α_c and b:

$$\mathrm{SPR}(a > 0) = \frac{16 - (1 - 3b)(1 - 3\cos^2\alpha_c)}{16 + 2(1 - 3b)(1 - 3\cos^2\alpha_c)} \tag{C1}$$

$$\mathrm{SPR}(a < 0) = \frac{8 + (1 - 3b)(1 - 3\cos^2\alpha_c)}{8 - 2(1 - 3b)(1 - 3\cos^2\alpha_c)}. \tag{C2}$$

If the chromophoric and diamagnetic species are identical, we see at once that SPR $\leq$ 1 for this model because the sign of the parameter a is the sign of $(1 - 3b)(1 - 3\cos^2\alpha_c)$. The numerators of Eqs. C1 and C2 are therefore always less than the denominators. As discussed in the text, any model predicting SPR $\leq$ 1 must be rejected on the basis of all experiments to date.

If the chromophoric and diamagnetic species are distinct, the α which determines the sign of a is distinct from α_c. If α and α_c are *both* < or >54.74°, SPR $\leq$ 1 for the reasons given in the preceding paragraph. Therefore, case (a) is of possible interest only when the chromophoric and diamagnetic species have considerably different tilt angles. (If both are near 54.74°, the SPR is near 1.) Consider two extreme cases, $\alpha_c \sim 0°$ and $\alpha_c \sim 90°$. The former is identical to case b with $\theta_y \sim 90°$ and is therefore not of separate interest. The latter describes a sufficiently unusual distribution that it deserves rejection on qualitative grounds. As $\alpha_c \sim 90°$, the vector $\mathbf{u}_c$ describing the normal to the molecule is lying near the plane of the membrane, and its azimuthal angle is taken random. But then the azimuthal angle θ_y of the transition moment is taken random about $\mathbf{u}_c$. Clearly this is a bad description of what would be better described as a totally random orientation of $\mathbf{y}$. We conclude, therefore, that virtually every application of case a is ruled out by experiment, common sense, or duplication by case b.

REFERENCES

1. GEACINTOV, N. E., F. VAN NOSTRAND, M. POPE, and J. B. TINKEL. 1971. Magnetic field effect on the chlorophyll fluorescence in *Chlorella*. *Biochim. Biophys. Acta.* **226**:263–269.
2. STACY, W. T., T. MAR, C. E. SWENBERG, and GOVINDJEE. 1971. An analysis of a triplet exciton model for the delayed fluorescence in *Chlorella*. *Photochem. Photobiol.* **14**:197–219.
3. AVAKIAN, P. 1974. Influence of magnetic fields on luminescence involving triplet excitons. *Pure Appl. Chem.* **37**:1–19.
4. GEACINTOV, N. E., and C. E. SWENBERG. 1978. Magnetic field effects in organic molecular spectroscopy. *In* Luminescence Spectroscopy. M. D. Lumb, editor. Academic Press, Inc. London. In press.
5. CAMPILLO, A. J., and S. L. SHAPIRO. 1976. Picosecond relaxation measurements in biology. Picosecond pulses. *Top. Appl. Phys.* **7**:000–000. SWENBERG, C. E., N. E. GEACINTOV, and M. POPE. 1976. Bimolecular quenching of excitons and fluorescence in the photosynthetic unit. *Biophys. J.* **16**:1447–1452.
6. See, e.g., HOFF, A. J. 1976. Kinetics of populating and depopulating of the components of the photo-induced triplet state of the photosynthetic bacteria *Rhodospirillum rubrum, Rhodopseudomonas spheroides. Biochim. Biophys. Acta.* **440**:765–771. VAN DER WALLS, J. H., and L. N. M. DUYSENS. 1977. On the magnetic field dependence of the yield of the triplet state in reaction centers of photosynthetic bacteria. *Biochim. Biophys. Acta.* **460**:547–554. NISSANI, E., A. SCHERZ, and H. LEVANON. 1977. The photoexcited triplet state of tetraphenyl chlorin, magnesium tetraphenyl porphyrin, and whole cells of *Chlamydamonas reinhardi*. A light modulation-EPR study. *Photochem. Photobiol.* **25**: 93–101.
7. ARNOLD, W., R. STEELE, and H. MUELLER. 1958. On the magnetic asymmetry of muscle fibers. *Proc. Natl. Acad. Sci. U. S. A.* **44**:1–4.
8. CHALAZONITIS, N., R. CHAGNEUX, and A. ARVANITAKI. 1970. Rotation des segments externes des photorecepteurs dans le champ magnetique constant. *C. R. Acad. Sci. Paris (D).* **271**:130–133.

9. GEACINTOV, N. E., F. VAN NOSTRAND, J. F. BECKER, and J. B. TINKEL. 1972. Magnetic field induced orientation of photosynthetic systems. *Biochim. Biophys. Acta.* **267**:65–79.
10. CLEMENT-METRAL, J. 1975. Direct observation of the rotation in a constant magnetic field of highly organized lamellar structures. *FEBS (Fed. Eur. Biochem. Soc.) Lett.* **50**:257–260.
11. SADLER, D. M. 1976. X-ray diffraction from chloroplast membranes oriented in a magnetic field. *FEBS (Fed. Eur. Biochem. Soc.) Lett.* **67**:289–293.
12. NEUGEBAUER, D-CH., A. E. BLAUROCK, and D. L. WORCESTER. 1977. Magnetic orientation of purple membranes demonstrated by optical measurements and neutron scattering. *FEBS (Fed. Eur. Biochem. Soc.) Lett.* **78**:31–35.
13. VAN NOSTRAND, F. 1972. The *in vivo* orientation of chlorophyll: a spectroscopic study of magnetically oriented photosynthetic systems. Ph.D. thesis, New York University.
14. BECKER, J. F., N. E. GEACINTOV, F. VAN NOSTRAND, and R. VAN METTER. 1973. Orientation of chlorophyll *in vivo:* studies with magnetic field oriented Chlorella. *Biochem. Biophys. Res. Commun.* **51**: 597–602.
15. GEACINTOV, N. E., F. VAN NOSTRAND, and J. F. BECKER. 1974. Polarized light spectroscopy of photosynthetic membranes in magneto-oriented whole cells and chloroplasts: fluorescence and dichroism. *Biochim. Biophys. Acta.* **347**:443–463.
16. BECKER, J. F. 1975. Study of biological membranes oriented in a homogeneous magnetic field. Ph.D. thesis, New York University.
17. BRETON, J., M. MICHEL-VILLAZ, and G. PAILLOTIN. 1973. Orientation of pigments and structural proteins in the photosynthetic membrane of spinach chloroplasts: a linear dichroism study. *Biochim. Biophys. Acta.* **314**:42–56.
18. GOEDHEER, J. C. 1955. Orientation of the pigment molecules in the chloroplast. *Biochim. Biophys. Acta.* **16**:471–476.
19. BECKER, J. F., F. TRENTACOSTI, and N. E. GEACINTOV. 1978. A linear dichroism study of the orientation of aromatic protein residues in magnetically oriented bovine rod outer segments. *Photochem. Photobiol.* **27**:51–54.
20. WORCESTER, D. L. August 1977. Structural origins of diamagnetic anisotropy in proteins. AERE Harwell report MPD/NBS/36.
21. PARK, R. B. 1965. Chloroplast structure. *In* The Chlorophylls. L. P. Vernon and G. R. Seely, editors. Academic Press, Inc., New York. 292.
22. SETLOW, R. B., and E. C. POLLARD. 1962. Molecular Biophysics. Addison-Wesley Publishing Company Inc., Reading Mass. 16.
23. KAMEN, M. D. 1963. Primary Process in Photosynthesis. Academic Press, Inc., New York. Chap. II.
24. LONSDALE, K. 1936. Magnetic anisotropy and electronic structure of aromatic molecules. *Proc. R. Soc. Lond. Math. Phys. Sci.* **A159**:149–161.
25. See, e.g., HONG, F., D. MAUZERALL, and A. MAURO. 1971. Magnetic anisotropy and the orientation of retinal rods in a homogeneous magnetic field. *Proc. Natl. Acad. Sci. U. S. A.* **68**:1283–1285.
26. PLATT, J. R. 1949. Classification of spectra of cata-condensed hydrocarbons. *J. Chem. Phys.* **17**:484–495. PLATT, J. R. 1950. Molecular orbital predictions of organic spectra. *J. Chem. Phys.* **18**:1168–1173.
27. SELWOOD, P. W. 1956. Magnetochemistry. John Wiley Interscience, New York. 2nd edition. Chap. VI, p. 28.
28. PAILLOTIN, G., and J. BRETON. 1977. Orientation of chlorophylls within chloroplasts as shown by optical and electrochromic properties of the photosynthetic membrane. *Biophys. J.* **18**:63–79.
29. MICHEL-VILLAZ, M. 1976. Fluorescence polarization: pigment orientation and energy transfer in photosynthetic membranes. *J. Theor. Biol.* **58**:113–129.
30. VAN METTER, R. L. 1977. Excitation energy transfer in the light-harvesting chlorophyll-a/b protein. *Biochim. Biophys. Acta.* **462**:642–658. KNOX, R. S., and R. L. VAN METTER. 1978. Fluorescence of light-harvesting chlorophyll-a/b protein complexes: implications for the photosynthetic unit. *Ciba Symp.* **61.** In press.
31. ABRAMOWITZ, M., and I. A. STEGUN. 1965. Handbook of Mathematical Functions. Dover Publications Inc., New York. 276–298.